Homogenization Technique for Axially Laminated Rotors of Synchronous Reluctance Machines

Floran Martin, Anouar Belahcen, Antti Lehikoinen, and Paavo Rasilo
Aalto University, Department of Electrical Engineering and Automation, Otakaari 5, 02150 Espoo, Finland

In this paper, we propose a homogenization technique to model the axially laminated rotor of synchronous reluctance machines. Thus, the computational effort can be significantly reduced by replacing the laminated parts of the rotor by some equivalent anisotropic media. The proposed method is validated in terms of flux density and electromagnetic torque. Some small discrepancies can be noticed due to the air-gap fluctuations caused by the steel sheets and the interlaminar insulation sheets of the rotor. With the test machine, the homogenization method reduces by the number of elements to one fourth and the computation time to one third.

Index Terms—**Electromagnetic torque, finite element analysis, homogenization technique, magnetic fields, magnetic flux, reluctance motors, synchronous machines**

I. Introduction

AXIALLY laminated synchronous reluctance machines have received growing interest in recent years [1], [2]. Due to their inherent simplicity and low cost, these machines are viable candidates for various general applications with adjustable speed. With axially laminated rotors, sychronous reluctance machines increase the electromagnetic torque by raising their saliency ratio [1], [2]. Moreover, their quite smooth rotor decreases significantly air friction losses which are of great significance for high speed applications [3], [4]. The construction of the axially laminated rotor consists of assembling a stack of steel laminations with interlaminar insulation sheets in order to enhance the saliency ratio with differing reluctances on direct and quadrature axes. Nonmagnetic bolts and pole holders are mounted to fix the laminations. The stack of steel laminations can be composed of non-oriented steel or grain-oriented steel. With grain oriented laminations, the efficiency is slightly higher but the core losses in stator and rotor also increase [5].

The calculation of magnetic quantities such as the electromagnetic torque can be performed with analytical models [1], [6] or numerical methods [1], [5], [7]. The finite element method is generally applied when a high degree of accuracy is needed, but it requires a detailed characterization of the geometry [6], [7]. Every steel lamination and interlaminar insulation sheet are discretized into finite elements. When the lamination thickness is small compared to the rotor radius, the computational effort is huge because the rotor geometry discretization contains a high number of nodes and elements.

In this paper, we propose to reduce the computational effort and time by modeling the axially laminated rotor parts with a homogenization technique so that a coarser mesh can be used to discretize the axial laminations. Usually, homogenization methods are applied on the stator windings [8], or on test iron stacks [9], [10], [11], [12]. Thus, the homogenization technique involves both magnetic and electric properties of the different materials. In case the thickness of the axial laminations is lower than twice the smallest skin depth, the eddy current flowing in these laminations can be neglected [13] and so the axially laminated parts can be homogenized only in terms of magnetic properties. In this paper, the homogenization technique of the axially laminated parts is first detailed, then the finite element method is briefly described. Finally, the homogenization method is validated in terms of air gap flux density components and electromagnetic torque by comparing computations for models of fully laminated rotor parts and homogenized rotor parts.

Manuscript received March 20, 2015; revised ?? ??, 2015. Corresponding author: F. Martin (email: floran.martin@aalto.fi).

II. Method of analysis

A. Homogenization technique

The stack of steel sheets with interlaminar insulation sheets is homogenized and the constitutive relation between magnetic quantities is derived. This stack of laminations can be homogenized with an anisotropic medium (Fig. 1).

Its equivalent reluctivity can be calculated by considering a serial and a parallel association of both the steel sheets and the insulation sheets, respectively for the lamination direction $\vec{u}$ and the orthogonal direction $\vec{v}$ of the lamination [12]. The magnetic field components, h_u and h_u, in the homogeneous medium can be computed by:

$$\begin{aligned} h_u\left(b_u\right) &= \frac{\nu_0\,\nu_i(b_u)}{(1-\alpha)\,\nu_i(b_u)+\alpha\,\nu_0}b_u \\ h_v\left(b_v\right) &= \alpha\,\nu_i(b_v)\,b_v+(1-\alpha)\,\nu_0\,b_v \end{aligned} \tag{1}$$

where b_u and b_v are the components of the magnetic flux density in the lamination coordinate system, ν_i is the reluctivity of the steel sheet with the reluctivity of the interlaminar insulation sheets considered as the reluctivity of vacuum ν_0, and α is the ratio of steel laminations in the stack.

This article has been accepted for publication in a future issue of this journal, but has not been fully edited. Content may change prior to final publication. Citation information: DOI 10.1109/TMAG.2015.2463262, IEEE Transactions on Magnetics

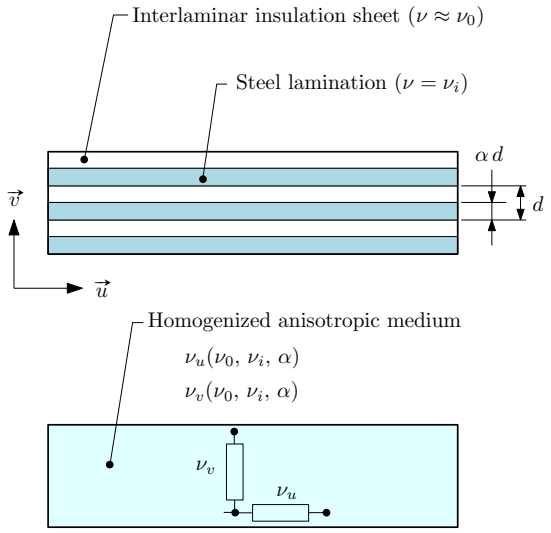

Fig. 1. Principle of homogenization of a stack of steel sheets with interlaminar insulation sheets. Upper figure shows the fully laminated model, lower one presents the homogenized model. ν is the reluctivity of the material with the index i as iron, u and v indices relate to the respective directions.

B. Finite element method

The cross section $\mathcal{S}$ of the axially laminated synchronous reluctance machine is discretized into second order trianglular elements and the magnetostatic problem is formulated in terms of the magnetic vector potential $\mathbf{A}$. Within the considered 2D geometry, the axial component of the magnetic vector potential A is governed by the partial differential equation given by:

$$\nabla \times \nu \nabla \times (A\, e_z) = J\, e_z \tag{2}$$

where ν is the reluctivity depending on both the considered region and the components of the magnetic flux density, J is the current density source in the conductors, and e_z the unit vector in the $\vec{z}$ direction.

This equation is solved with the Galerkin's method by minimizing the energy functional $\mathcal{F}$ given by [14]:

$$\mathcal{F} = \int_{\mathcal{S}} \left[\int_0^{\boldsymbol{B}} \boldsymbol{H}^{\mathrm{T}} d\boldsymbol{B} - \boldsymbol{J}^{\mathrm{T}} \boldsymbol{A} \right] dS \tag{3}$$

where $\boldsymbol{B}$ and $\boldsymbol{H}$ are the magnetic flux density and the magnetic field respectively.

Since iron based regions are non-linear, this energy functional is also non-linear and its minimization requires an iterative process. The estimated magnetic vector potential $\mathbf{A}_k$ is updated after each k iteration with the Newton-Raphson method. Its expression is given by:

$$\boldsymbol{A}_{k+1} = \boldsymbol{A}_k - {\mathbf{P}_k}^{-1} \boldsymbol{R}_k \tag{4}$$

where the residual vector $\boldsymbol{R}$ and the Jacobian matrix $\mathbf{P}$ are composed of the terms given by:

$$R_i = \int_{\mathcal{S}} \nabla \times (N_i\, e_z)^{\mathrm{T}}\, \boldsymbol{H} - J_i\, N_i\, dS$$

$$P_{i\,j} = -\int_{\mathcal{S}} \nabla \times (N_i\, e_z)^{\mathrm{T}} \left[\frac{\partial \mathbf{H}}{\partial \mathbf{B}} \right] \nabla \times (N_j\, e_z)\, dS \tag{5}$$

with N_i the shape function of the finite element method, i and j are node numbers.

Except for homogenized region, every material is considered isotropic so the incremental reluctivity tensor $\partial\mathbf{H}/\partial\mathbf{B}$ is a diagonal matrix. Within the homogenous anisotropic media, the magnetic field components h_u and h_v are expressed in the lamination coordinate system (O, $\vec{u}$, $\vec{v}$). In order to implement the homogenized model, we should express these magnetic field components in the global coordinate system (O, $\vec{x}$, $\vec{y}$). Since the homogeneous media are located in the rotor, the relation between the lamination direction $\vec{u}$ and the $\vec{x}$ axis depends on the angular position of the rotor. Moreover, in case the lamination sheets are bended, the lamination direction can be considered as the tangent of the curved lamination and this relation also depends on the coordinate of the integration points (Fig. 2). Thus, we can calculate h_x and h_y by rotating the magnetic field components h_u and h_v :

$$\begin{bmatrix} h_x \\ h_y \end{bmatrix} = \mathcal{R}(\theta) \begin{bmatrix} h_u \\ h_v \end{bmatrix} = \begin{bmatrix} \cos\theta & \sin\theta \\ -\sin\theta & \cos\theta \end{bmatrix} \begin{bmatrix} h_u \\ h_v \end{bmatrix} \tag{6}$$

where θ is the angle between the $\vec{x}$ axis and the lamination direction $\vec{u}$.

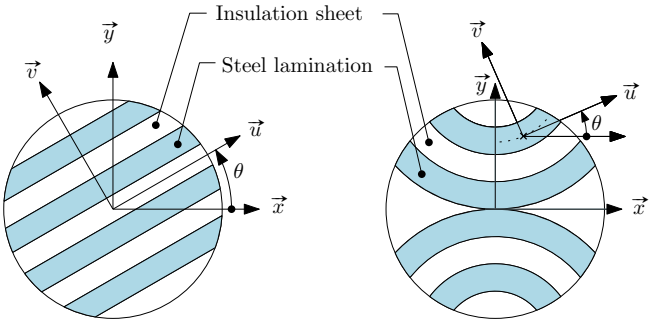

Fig. 2. Relation between the lamination coordinate system (O, $\vec{u}$, $\vec{v}$) and the global coordinate system (O, $\vec{x}$, $\vec{y}$). The left figure presents a rotor at an arbitrary angular position with straight lamination. The right figure shows a rotor with curved lamination.

The incremental reluctivity tensor is calculated with a similar manner by:

$$\begin{bmatrix} \dfrac{\partial h_x}{\partial b_x} & \dfrac{\partial h_x}{\partial b_y} \\ \dfrac{\partial h_y}{\partial b_x} & \dfrac{\partial h_y}{\partial b_y} \end{bmatrix} = \mathcal{R}(\theta) \begin{bmatrix} \dfrac{\partial h_u}{\partial b_u} & 0 \\ 0 & \dfrac{\partial h_v}{\partial b_v} \end{bmatrix} \mathcal{R}^{\mathrm{T}}(\theta) \tag{7}$$

The Newton-Raphson method converges if the incremental reluctivity tensor is positive definite.

This article has been accepted for publication in a future issue of this journal, but has not been fully edited. Content may change prior to final publication. Citation information: DOI 10.1109/TMAG.2015.2463262, IEEE Transactions on Magnetics

C. Torque calculation

With constant flux Ψ, ie. constant magnetic vector potential, the electromagnetic torque Γ_{emg} can be determined by differentiating the magnetic energy W_{mag} with respect to the rotor displacement ϕ by :

$$\Gamma_{emg} = -\frac{\partial W_{mag}}{\partial \phi}\bigg|_{\Psi=constant} \tag{8}$$

With a similar method described in [15], [16], the electromagnetic torque is computed in the air-gap with the method of virtual displacement with constant magnetic vector potential :

$$\Gamma_{emg} = \nu_0 L \sum_{e=1}^{N_{ag}} \int_{\mathcal{S}_e} \boldsymbol{B}^{\mathrm{T}} \tilde{\mathbf{G}}^{-1} \frac{\partial \tilde{\mathbf{G}}}{\partial \phi} \boldsymbol{B} |\mathbf{G}| - \frac{1}{2} \boldsymbol{B}^2 \frac{\partial |\mathbf{G}|}{\partial \phi} \, dS \tag{9}$$

where L is the active length of the machine, N_{ag} is the number of elements in the air-gap layer, $\mathbf{G}$ is the Jacobian matrix of the transformation from (x, y) coordinate to (ξ, η) coordinate of the reference triangle, $|\mathbf{G}|$ is its determinant, and $\mathcal{S}_e$ is the surface of the reference triangular element. $\tilde{\mathbf{G}}$ is defined for isoparametric transformation by :

$$\tilde{\mathbf{G}} = \sum_{i=1}^{N_p} \begin{bmatrix} \frac{\partial N_i}{\partial \xi} y_i & -\frac{\partial N_i}{\partial \xi} x_i \\ \frac{\partial N_i}{\partial \eta} y_i & -\frac{\partial N_i}{\partial \eta} x_i \end{bmatrix} \tag{10}$$

where N_p is the number of nodes in the trianglular element ($N_p = 6$ for second order triangles).
The differentiations $\partial \tilde{\mathbf{G}}/\partial \phi$ are calculated by :

$$\frac{\partial \tilde{\mathbf{G}}}{\partial \phi} = \sum_{i=1}^{N_p} \begin{bmatrix} \frac{\partial N_i}{\partial \xi} \frac{\partial y_i}{\phi} & -\frac{\partial N_i}{\partial \xi} \frac{\partial x_i}{\phi} \\ \frac{\partial N_i}{\partial \eta} \frac{\partial y_i}{\phi} & -\frac{\partial N_i}{\partial \eta} \frac{\partial x_i}{\phi} \end{bmatrix} \tag{11}$$

The differentiation of the determinant of the Jacobian with respect to the virtual displacement can easily be computed with the terms of $\mathbf{G}$ and $\partial \tilde{\mathbf{G}}/\partial \phi$.

In case all the nodes of one element are virtually moving from the same angle, the terms of $\partial \tilde{\mathbf{G}}/\partial \phi$ and $\partial |\mathbf{G}|/\partial \phi$ become nil so only the elements which contain at least one moving node and not all of them can be considered to compute the electromagnetic torque. This means that only distorted elements from the air-gap are needed in this computation. In our models, these elements are confined within a predefined layer located in the middle of the air-gap.

III. Results and Discussion

In order to validate the proposed method, an axially laminated synchronous reluctance machine is analyzed by modeling both a fully laminated rotor and a homogenized anisotropic rotor with the same mesh for different load angles and the same current density. The machine is meshed with 40 888 second order triangles and 81 802 nodes, among which 37 435 nodes are in the rotor. The main parameters of the test machine are reported in Table I.

TABLE I
Parameters of the Test Machine

Number of pole pairs	1
Number of phases	3
Outer radius of the stator core [mm]	137.5
Core length [mm]	148.5
Inner radius of the stator [mm]	63.25
Outer radius of the rotor [mm]	60.94
Number of stator slots	36
Thickness of rotor lamination [mm]	5
Ratio of steel in the lamination	0.6
Applied current per phase [A]	6.64

A. Magnetic flux density

In Figs. 3-5, we can notice that the flux lines follow the same direction in both models. The amplitude of the flux density in the homogenized rotor is equal to the average flux density in the steel sheets and the interlaminar insulation sheets. Moreover, the amplitude of the magnetic flux density presents similar values in the stator. Besides the fact that the flux line and the average flux density are the same, in Fig. 4, the anisotropy effect can be appreciated in the behavior of the magnetic flux. In Fig. 5, the stator windings produces flux in the transverse direction of the rotor stack that heavily reduces the total flux in the machine. Results of homogenized and non-homogenized models are very similar.

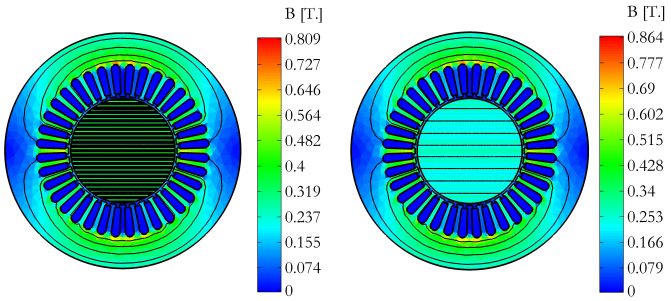

(a) Laminated rotor (b) Homogeneous rotor

Fig. 3. Flux density amplitude and flux lines in the reluctance machine with rotor at 0 deg. The flux lines follow the same direction in both models. The amplitude of the flux density in the homogenized case is equal to the average flux density in the full model.

In Figs. 6-8, we can notice that the components of the magnetic flux density in the middle of the air-gap are similar with the homogeneous rotor and the axially laminated rotor. However, the air gap flux density computed with the fully modeled laminations presents some small additional fluctuations. They are caused by the magnetic air-gap variations due to the alternation of the steel sheets and the insulation sheets. Since the homogenization technique does not consider this phenomenon, the air-gap flux density does not include these small fluctuations in this case. In Fig. 9, we can perceive that, for 45 deg. of load angle, the circumferential components of magnetic flux density presents some higher difference (29.6 %) than the radial component (19.2 %).

This article has been accepted for publication in a future issue of this journal, but has not been fully edited. Content may change prior to final publication. Citation information: DOI 10.1109/TMAG.2015.2463262, IEEE Transactions on Magnetics

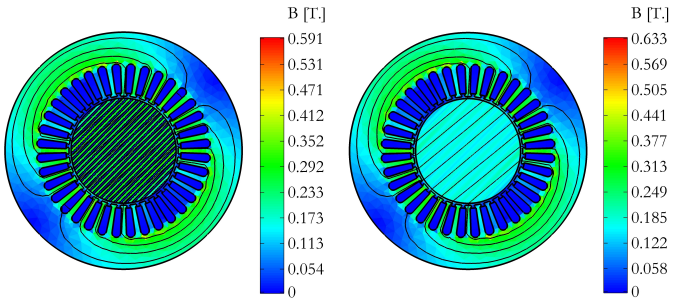

(a) Laminated rotor (b) Homogeneous rotor

Fig. 4. Flux density amplitude and flux lines in the reluctance machine with rotor at 45 deg. Besides the fact that the flux lines and the average flux are the same, the anisotropy effect can be observed in the behavior of the flux.

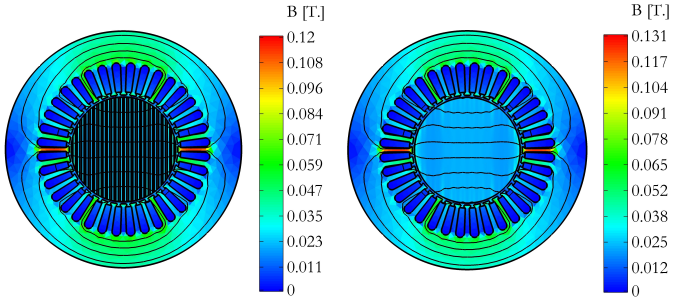

(a) Laminated rotor (b) Homogeneous rotor

Fig. 5. Flux density amplitude and flux lines in the reluctance machine with rotor at 90 deg. The fact that the stator produced flux is now in the transverse direction of the rotor stack reduces heavily the total flux in the machine.

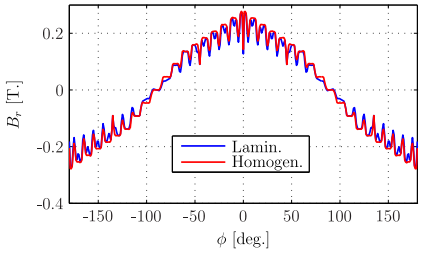

(a) Radial component of the magnetic flux density

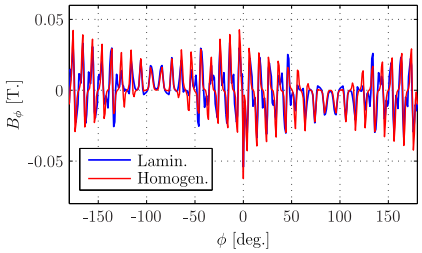

(b) Circumferential component of the magnetic flux density

Fig. 6. Flux density components in the air-gap with rotor at 0 deg. Except for the high spatial harmonic caused by the rotor laminations, the results of the homogenized and full models are very similar.

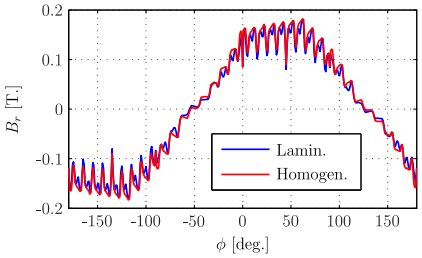

(a) Radial component of the magnetic flux density

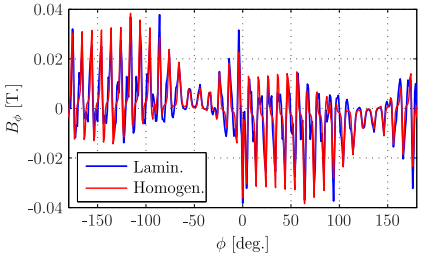

(b) Circumferential component of the magnetic flux density

Fig. 7. Flux density components in the air-gap with rotor at 45 deg. Increasing the load ange causes a decrease of air-gap flux density, which is correctly modeled by both the homogenized and the full model.

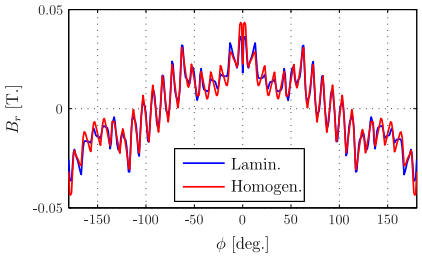

(a) Radial component of the magnetic flux density

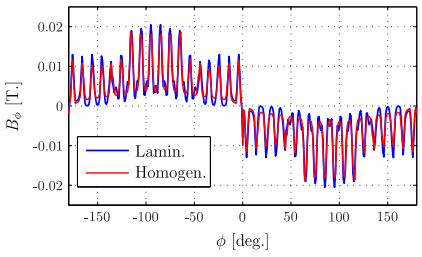

(b) Circumferential component of the magnetic flux density

Fig. 8. Flux density components in the air-gap with rotor at 90 deg. The flux practically does not flow as it has to go along the lowest reluctivity direction corresponding to the transverse lamination. Once more, the homogenized model takes correctly this effect into account.

In Fig. 7, increasing the load angle causes a decrease of the air-gap flux density, which is correctly modeled by both the homogenized and the full model. In Fig. 8, the flux practically does not flow as it has to go along the lowest reluctivity direction corresponding to the transverse lamination. Once more the homogenized model takes correctly this effect into account.

This article has been accepted for publication in a future issue of this journal, but has not been fully edited. Content may change prior to final publication. Citation information: DOI 10.1109/TMAG.2015.2463262, IEEE Transactions on Magnetics

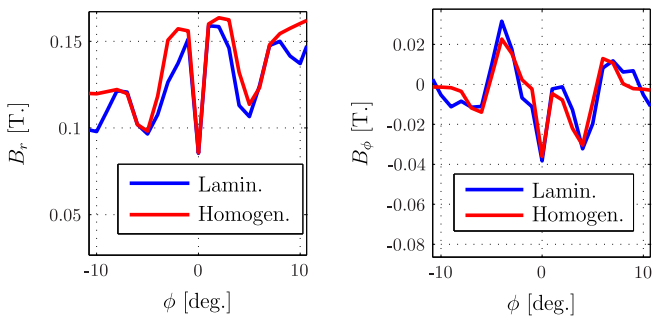

(a) Radial component (b) Circumferential component

Fig. 9. Zoom of the flux density components in the air-gap with rotor at 45 deg. Some bigger discrepancies are reached for the circumferential components (29.6 %). The radial component presents at maximum a relative error of 19.2 %.

B. Electromagnetic torque

The electromagnetic torque was computed in the air-gap of the axially laminated synchronous reluctance machine for different rotor positions, from -90° to 90° by step of 5 °. With the method of virtual displacement described in II-C, it is important that the virtually moving elements remain the same for any rotor position, so the torque is computed in an annulus layer of the air-gap [16].

In Fig. 10, we can notice that the electromagnetic torque presents the well-known torque sinusoidal dependance on the load angle. Moreover, the rotor with fully modeled laminations and the homogeneous rotor with the same mesh and a coarse mesh present similar torque computations regardless the fact that the coarse mesh presents one fourth of elements. Furthermore, the difference in the torque computation between homogenized and non-homogenized models is only 8.02 % at its maximum. These discrepancies are mainly caused by the magnetic air-gap fluctuations due to alternation of the steel sheets and the interlaminar insulation sheets that were neglected in the homogenized medium.

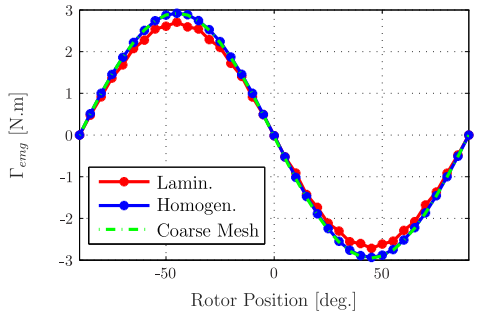

Fig. 10. Electromagnetic torque for different rotor positions. The homogenized models compute the torque with similar accuracy regardless of the fact that one of them has half the numbers of elements. Furthermore, the difference between homogenized and non-homogenized computation is only 8% at its maximum.

In Table II, the accuracy and computation time of the torque computation are compared for the rotor with fully modeled laminations and for the homogeneous rotor with the same mesh and a coarse mesh. With the same mesh, the computation time with the homogeneous rotor is slightly larger than with the fully modeled laminations. This can be explained because more elements are non-linear in the homogenized rotor compared with the fully modeled laminations composed of interlaminar insulation sheets which are linear. However, since the homogeneous rotor can be discretized with a coarse mesh, the number of elements can be reduced to one fourth and the computation time can be reduced to one third. Moreover, the accuracy of the torque computation remains similar with a coarse mesh and with the fully laminated mesh. Thus, most of the discrepancies arise from the neglected magnetic air-gap fluctuations due to the alternation of the steel sheets and the interlaminar insulation sheets.

TABLE II
COMPARISON OF MODELS ACCURACY AND THEIR COMPUTATION TIMES

Rotor model	Number of elements	Number of nodes	Computation time [s.]	Relative error [%]
Fully modeled laminations	40 888	81 802	153.56	0
Homogeneous with fully laminated mesh	40 888	81 802	178.41	8.02
Homogeneous with coarse mesh	10 000	20 076	51.57	8.53

These magnetic air-gap fluctuations are mainly depending on the steel ratio α of the lamination stack. The figure 11 shows the impact of this ratio on the electromagnetic torque for a load angle of 45 deg. First, we can notice that the maximum electromagnetic torque is reached for 60 % of steel in the lamination stack. With this ratio, the relative error between homogenized and non-homogenized computation is 7.93 % only. When the steel ratio is either 0 or 1, the electromagnetic torque should be nil since the smooth rotor would be composed of exclusively interlaminar insulating material or steel respectively. In those cases, the inductance in the direct axis would be equal to the inductance in the quadratic axis, resulting in a nil reluctance torque. Finally, we can perceive that the torque discrepancies (27.4 %) between homogenized and non-homogenized computation are maximum with a steel ratio of 20 %. Even if this relative error is quite small, it would be reasonable to keep the steel ratio near 50 % since the design of an axially laminated synchronous rotor aims to increase the ratio between the quadratic and the direct inductances.

IV. Conclusion

In this paper, we proposed a homogenization technique for an axially laminated rotor of a synchronous reluctance machine. The axially laminated rotor is represented by an equivalent anisotropic medium in order to ease the computational effort. The proposed method was validated by

comparing the flux density and the electromagnetic torque computed with laminated and homogeneous rotors. Even if some small discrepancies were noticed due to the alternation of the steel sheets and the interlaminar insulation sheets, the components of the flux density and the electromagnetic torque can be accurately predicted with the homogenization method. Moreover, the computation time can be reduced to one third with the test machine when the homogeneous parts of the rotor are discretized with a coarse mesh.

In future work, the homogenization technique will be improved by considering the magnetic air-gap fluctuations due to the alternation of the steel sheets and the interlaminar insulation sheets. These fluctuations could be taken into account by modulating the components of the magnetic flux density in the air-gap by a relative air-gap permeance. Moreover, the homogeneous model will be included in an optimization process for design purpose.

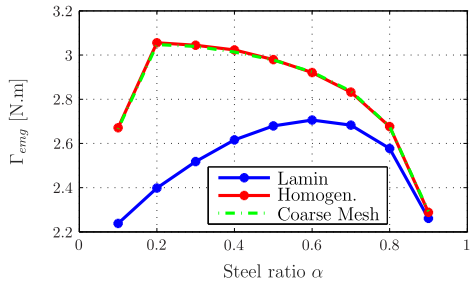

Fig. 11. Electromagnetic torque for different steel ratio α in the stack at the same rotor position of 45 °. The maximum torque is reached with α = 0.6. For this ratio, the relative error between homogenized and non-homogenized computation is 7.93 %. However, the relative error increases for lower steel ratio until 27.4% that is reached for α = 0.2.

ACKNOWLEDGMENT

The research leading to these results has received funding from the European Research Council under the European Union's Seventh Framework Programme (FP7/2007-2013) / ERC grant agreement n°339380. The Academy of Finland is acknowledged for financial support.

REFERENCES

[1] N. Bianchi and B. Chalmers, "Axially laminated reluctance motor: analytical and finite-element methods for magnetic analysis," *IEEE Trans. Magn.*, vol. 38, no. 1, pp. 239–245, Jan 2002.

[2] Y. H. Kim, J. H. Lee, and J. K. Lee, "Optimum design of axially laminated anisotropic rotor synchronous reluctance motor for torque density and ripple improvement," in *Computation in Electromagnetics (CEM 2014), 9th IET International Conference on*, March 2014, pp. 1–2.

[3] A. Arkkio, T. Jokinen, and E. Lantto, "Induction and permanent-magnet synchronous machines for high-speed applications," in *Proceedings of the 8th Internationnal Conference on Electrical Machines and Systems*. ICEMS 2005, 2005, pp. 871–876.

[4] M. Lamghari-Jamal, "Modélisation magnéto-thermique et optimisation de machines rapides," Ph.D. dissertation, Université de Nantes, 2006.

[5] F. Isaac, A. Arkadan, and A. El-Antably, "Characterization of axially laminated anisotropic-rotor synchronous reluctance motors," *IEEE Trans. Energy Convers.*, vol. 14, no. 3, pp. 506–511, Sep 1999.

[6] E. Obe, "Calculation of inductances and torque of an axially laminated synchronous reluctance motor," *Electric Power Applications, IET*, vol. 4, no. 9, pp. 783–792, Nov 2010.

[7] F. Isaac, A. Arkadan, and A. El-Antably, "Magnetic field and core loss evaluation of ala-motor synchronous reluctance machines taking into account material anisotropy," *IEEE Trans. Magn.*, vol. 34, no. 5, pp. 3507–3510, Sep 1998.

[8] G. Meunier, V. Charmoille, C. Guerin, P. Labie, and Y. Marechal, "Homogenization for periodical electromagnetic structure: Which formulation?" *IEEE Trans. Magn.*, vol. 46, no. 8, pp. 3409–3412, Aug 2010.

[9] P. Dular, J. Gyselinck, C. Geuzaine, N. Sadowski, and J. Bastos, "A 3-d magnetic vector potential formulation taking eddy currents in lamination stacks into account," *IEEE Trans. Magn.*, vol. 39, no. 3, pp. 1424–1427, May 2003.

[10] P. Dular, J. Gyselinck, and L. Krhenbhl, "A time-domain finite element homogenization technique for lamination stacks using skin effect subbasis functions," *COMPEL - The international journal for computation and mathematics in electrical and electronic engineering*, vol. 25, no. 1, pp. 6–16, 2006.

[11] L. Cheng, S. Sudo, Y. Gao, H. Dozono, and K. Muramatsu, "Homogenization technique of laminated core taking account of eddy currents under rotational flux without edge effect," *IEEE Trans. Magn.*, vol. 49, no. 5, pp. 1969–1972, May 2013.

[12] H. Kaimori, A. Kameari, and K. Fujiwara, "Fem computation of magnetic field and iron loss in laminated iron core using homogenization method," *IEEE Trans. Magn.*, vol. 43, no. 4, pp. 1405–1408, April 2007.

[13] F. Martin, M. E. Zaim, A. Tounzi, and N. Bernard, "Improved analytical determination of eddy current losses in surface mounted permanent magnets of synchronous machine," *IEEE Trans. Magn.*, vol. 50, no. 6, pp. 1–9, June 2014.

[14] G. Meunier, *The Finite Element Method for Electromagnetic Modeling*. Wiley-ISTE, 2008.

[15] J. L. Coulomb, "A methodology for the determination of global electromechanical quantities from a finite element analysis and its application to the evaluation of magnetic forces, torques and stiffness," *IEEE Trans. Magn.*, vol. 19, no. 6, pp. 2514–2519, Nov 1983.

[16] B. Silwal, P. Rasilo, L. Perkkio, M. Oksman, A. Hannukainen, T. Eirola, and A. Arkkio, "Computation of torque of an electrical machine with different types of finite element mesh in the air gap," *IEEE Trans. Magn.*, vol. 50, no. 12, pp. 1–9, Dec 2014.